



Original Article

Cognitive MRI-TRUS fusion-targeted prostate biopsy according to PI-RADS classification in patients with prior negative systematic biopsy results

Wei-Jen Lai ^{a,b}, Hsin-Kai Wang ^{a,b}, Hsian-Tzu Liu ^{a,b}, Byung Kwan Park ^c, Shu-Huei Shen ^{a,b,d,*}, Tzu-Ping Lin ^{b,e}, Hsiao-Jen Chung ^{b,e}, Yi-Hsiu Huang ^{b,e}, Yen-Hwa Chang ^{b,e}

^a Department of Radiology, Taipei Veterans General Hospital, Taipei, Taiwan, ROC

^b National Yang-Ming University School of Medicine, Taipei, Taiwan, ROC

^c Department of Radiology, Samsung Medical Center, Sungkyunkwan University School of Medicine, Seoul, South Korea

^d National Yang-Ming University, Institute of Public Health, Taipei, Taiwan, ROC

^e Department of Urology, Taipei Veterans General Hospital, Taipei, Taiwan, ROC

Received December 17, 2015; accepted May 1, 2016

Abstract

Background: The purpose of this study was to evaluate the prostate cancer yield rate of targeted transrectal ultrasound (TRUS)-guided biopsy with cognitive magnetic resonance imaging (MRI) registration without concurrent systematic biopsy in patients with previous negative systematic TRUS-guided biopsy results and persistently elevated prostate-specific antigen (PSA) levels.

Methods: In this prospective study conducted from August 2013 to January 2015, patients with at least one previous negative systematic TRUS-guided biopsy and persistently high PSA (≥ 4 ng/mL) levels were referred for multiparametric MRI (mpMRI). Those patients with suspicious findings on mpMRI received a subsequent cognitive MRI-TRUS fusion biopsy. The cancer-detection rate, tumor location, and Gleason score were confirmed, and PSA-related data were compared between cancer-yield and noncancer-yield groups.

Results: In total, 48 patients were included in this study. MRI was designated to be four and five in 17 patients. Fifteen patients received a cognitive fusion-targeted biopsy, and prostate cancers were detected in 10 patients. The cancer-detection rate was 20.8% (10/48), and the positive-predictive value of MRI was 66.7%. No significant differences were observed in the PSA level, PSA velocity, or transitional zone volume between the cancer-yield and noncancer-yield groups; however, the corresponding difference in PSA transitional zone density was significant ($p = 0.025$).

Conclusion: Cognitive MRI-TRUS fusion-targeted biopsy without concurrent systematic biopsy can detect significant prostate cancer in patients with previous negative systematic biopsy results and persistently elevated PSA levels. Noncancer-yield patients should undergo active surveillance and further follow-ups.

Copyright © 2016, the Chinese Medical Association. Published by Elsevier Taiwan LLC. This is an open access article under the CC BY-NC-ND license (<http://creativecommons.org/licenses/by-nc-nd/4.0/>).

Keywords: image-guided biopsy; magnetic resonance imaging; prostate; prostate cancer; prostate-specific antigen

1. Introduction

In Taiwan, the incidence rate of prostate disease has elevated along with increases in the aging population.¹ The prostate-specific antigen (PSA) test is a fast and convenient method for prostate-cancer screening and is widely used. The PSA test has a high level of sensitivity, but low specificity for prostate cancer. Many benign prostate diseases, including

Conflicts of interest: The authors declare that they have no conflicts of interest related to the subject matter or materials discussed in this article.

* Corresponding author. Dr. Shu-Huei Shen, Department of Radiology, Taipei Veterans General Hospital, 201, Section 2, Shih-Pai Road, Taipei 112, Taiwan, ROC.

E-mail address: shshen@vghtpe.gov.tw (S.-H. Shen).

<http://dx.doi.org/10.1016/j.jcma.2016.05.004>

1726-4901/Copyright © 2016, the Chinese Medical Association. Published by Elsevier Taiwan LLC. This is an open access article under the CC BY-NC-ND license (<http://creativecommons.org/licenses/by-nc-nd/4.0/>).

prostatitis and benign prostatic hyperplasia (BPH), lead to an elevated PSA level.² For patients with elevated PSA levels, transrectal ultrasound (TRUS)-guided biopsy is the standard procedure for diagnosing prostate cancer; however, this is an invasive procedure with considerable complications, including infection, bleeding, and voiding difficulty.³ Furthermore, a high false-negative rate (39–52%) was reported for systematic prostate biopsy.⁴ Because the PSA test is used more frequently, the number of patients with an increased PSA level, but a negative prostate biopsy, is high, leading to difficulties in clinical management and causing patient anxiety and possible treatment delays. Considering the unreliability of the PSA test and systematic TRUS-guided prostate biopsy in diagnosing prostate cancer, advanced diagnostic methods for visualizing and subsequently guiding biopsies are imperative to improved patient care.

Magnetic resonance imaging (MRI) is a direct and noninvasive method for pretreatment assessments of prostate cancer. Combining anatomical imaging (high resolution T2-weighted images) with functional imaging techniques, including diffusion-weighted imaging (DWI), dynamic contrast-enhanced (DCE) imaging, and MR spectroscopy [i.e., multiparametric MRI (mpMRI)], has significantly improved the diagnostic accuracy for prostate cancer by enabling tumor detection and localization.^{5–9} Many studies reported that MRI scans increased cancer-detection rates in patients with elevated PSA levels and negative systematic TRUS-guided biopsy reports^{4,10–15}; however, the technical parameters of mpMRI, criteria for selecting the lesions for targeted biopsy, and the targeting approach differ among these studies. Here, we evaluated the prostate cancer-yield rate of cognitive MRI-TRUS fusion-targeted biopsy for mpMRI-visible lesions in patients with elevated PSA levels and previous negative systematic TRUS-guided biopsy.

2. Methods

2.1. Patient recruitment

This institutional review board-approved prospective study recruited consecutive patients with elevated PSA levels (≥ 4 ng/mL) and at least one previous negative systematic TRUS-guided biopsy and referred them for an MRI scan at the urology clinic of our institution from August 2013 to January 2015. Patients with pacemaker implantation or other contraindications for MRI examinations were excluded, and informed consent was obtained from all patients.

2.2. Imaging protocol

All imaging studies were performed using a 3.0 T MRI scanner (MR750, GE Medical Systems, Milwaukee, WI, USA) and a body coil for transmission and a four-coil phased-array torso coil for reception. The MRI protocol conformed to the European Society of Urogenital Radiology (ESUR) guidelines.¹⁶ Axial T1-weighted spin-echo MR images (repetition time/echo time = 400/9 ms; matrix size = 320×224 ; field of

view = 16×16 cm; excitation numbers = 2; and slice thickness/gap = 3 mm/0 mm) were obtained for detecting intraglandular hemorrhage. Subsequent T2-weighted fast spin-echo MR images (repetition time/echo time = 3000–4000/90 ms; echo train length = 17; matrix size = 512×256 ; field of view = 16×16 cm; excitation numbers = 4; and slice thickness/gap = 3 mm/0 mm) were obtained in the axial, sagittal, and coronal planes of the prostate and seminal vesicles for identifying the prostate zonal anatomy, three-dimensional (3D) diameter of the transitional zone, and pathology. Axial diffusion-weighted single-shot echo-planar imaging using a sensitivity encoding technique (SENSE-DWI; repetition time/echo time = 8500/minimum ms; matrix size = 128×128 ; field of view = 16×16 cm; excitation numbers = 4; slice thickness/gap = 3 mm/0 mm; axial scan b-factor values = 0 and 1000 s/mm² for three directions of the gradient; sensitivity encoding (SENSE) reduction factor = 2) were subsequently performed, and the corresponding apparent diffusion-coefficient maps were generated. For the 3D DCE study, images were obtained with an interval between each phase of <10 s, and subtraction was routinely performed to facilitate interpretation.

2.3. MRI reporting

Two radiologists, one with >10-years (S.H.S) and the other with 2-years (H.T.L) experience in urogenital radiology, reviewed the images together and consensually identified suspicious lesions. The locations of the lesions were assigned according to the 27 regions-of-interests described in the Prostate Imaging Reporting and Data System (PI-RADS).¹⁶

The diameters of the transitional zone on the axial, sagittal, and coronal planes were recorded, and the transitional zone volume was approximated as the product of all three axial diameters and π divided by six. The transitional zone density for PSA (PSATZ) was calculated by dividing the PSA level by the transitional zone volume.

2.4. Cognitive MRI-TRUS fusion biopsy

Patients with suspicious lesions following mpMRI received a subsequent target biopsy. TRUS-guided biopsy was performed using an Acuson S3000 ultrasound system (Siemens Medical Solutions, Malvern, PA, USA) with an EC9-4 endocavitary transducer. The patient was placed in the left lateral decubitus position with bent knee. After sterilization, cognitive MR-targeted biopsy was performed under TRUS-guidance in axial scan. Cognitive registration of the suspicious area was localized through both gray scale and color Doppler images. The lesion was identified on the basis of the zonal anatomy described or imaging landmarks, including bladder neck, cyst, or hyperplastic nodules. A needle adapter was attached to the ultrasound transducer for placing the biopsy needle. An 18-gauge/20-cm spring-loaded biopsy needle (Temno Evolution; BD Biosciences, Franklin Lakes, NJ, USA) was used for biopsy. Lesion targeting and tissue acquisition were performed under continuous real-time ultrasound monitoring. Three needle passes were performed for each target lesion.

The option of systematic biopsy was informed and discussed with the patient. If there was agreement, systemic biopsy of 12 cores was subsequently performed on the patient after targeted biopsy. After biopsy, TRUS was performed to survey the entire prostate gland for identifying hematoma.

2.5. Statistical analyses

Clinical data on serial PSA levels, previous biopsy date(s), and pathology reports (including Gleason score) were recorded for each patient. The updated PI-RADS version 2 score was assigned for each lesion for analysis according to the consensus of the two radiologists.¹⁷ Epstein criteria were used to define clinically significant cancer: any Gleason pattern 4 or Gleason 3 + 3 disease with core length 50% and/or > two cores positive on the standard 12-core TRUS-guided biopsies. Clinically significant prostate cancer on fusion biopsy was defined as any Gleason pattern 7–10 and/or Gleason 6 disease and an MRI-visible lesion >0.5 cm³.^{17,18} The cancer-detection rate and positive-predictive value of the MRI scans were calculated. The transitional zone volume and PSA-related data considering PSA level, PSA velocity, and PSATZ were recorded. We used an independent sample *t* test (SPSS version 21.0 software; IBM, Armonk, NY, USA) to compare the PSA level, PSA velocity, transitional zone volume, and PSATZ between the cancer-yield and noncancer-yield groups. If the independent sample *t* tests differed significantly, we used the receiver operating characteristic curve (ROC) and Youden index to determine the cut-off value.

3. Results

Forty-eight patients were included in this study, with a mean age of 65.7 years (48–78 years).

3.1. MRI study

The MRI scan analysis resulted in a PI-RADS score ≤2 in 25 patients, PI-RADS score = 3 in six patients, PI-RADS score = 4 in five patients, and PI-RADS score = 5 in 12

Table 1
Clinical profiles of patients in the cancer-yield group.

No.	Age (y)	Location	PI-RADS (v2)	Biopsy result		Operation result	
				Gleason score	Gleason score	Stage	Stage
1	62	TZa	5	3 + 3	3 + 4	pT3a	pT3a
2	74	TZa	5	3 + 3	3 + 4	pT2c	pT2c
3	67	TZa	5	4 + 3	4 + 3	pT2c	pT2c
4	66	TZa	5	3 + 4	3 + 4	pT3a	pT3a
5	72	TZa	5	4 + 3	NA	NA	NA
6	57	PZa	4	3 + 4	3 + 4	pT3a	pT3a
7	59	PZpl	5	3 + 4	3 + 4	pT3a	pT3a
8	71	TZa	5	3 + 3	3 + 3	pT2c	pT2c
9	58	TZa	5	4 + 4	4 + 3	pT3a	pT3a
10	79	PZpl	5	4 + 3	NA	NA	NA

NA = not available (patients did not receive surgery); PI-RADS = Prostate Imaging Reporting and Data System; PZa = anterior peripheral zone; PZpl = posterior lateral peripheral zone; pT = posterior transitional zone; TZa = anterior transitional zone.

patients. Two PI-RADS score = 4 patients declined to receive a biopsy and opted for follow-up. The remaining 15 patients with PI-RADS ≥4 received a cognitive MRI-TRUS fusion biopsy, with cancer successfully detected in 10 patients (Table 1). The lesions were iso- or low echogenicity, and may have shown hypervascularity according to color Doppler study. The mean time between the previous biopsy and MRI for cognitive registration was 771 days (53–3141 days), and the mean time between MRI and systematic TRUS-guided biopsy was 25.1 days (1–84 days). The cancer-detection rate was 20.8% (10/48). Nine cancer-positive patients exhibited PI-RADS scores of 5, and one patient had a PI-RADS score of 4. The cancer-yield rates for patients with PI-RADS scores of 5 and 4 were 75% (9/12) and 33.3% (1/3), respectively. The positive-predictive value of the targeted biopsy was 66.7% (10/15), and the average size of the 10 detected lesions was 2.17 cm (1.0–3.9 cm). Eight of the 10 patients had lesions in the anterior part of the prostate gland (Figs. 1 and 2), and two patients had lesions in the posterior lateral peripheral zone.

3.2. Pathology

Of the 10 cancer patients, three, three, three, and one patient showed Gleason scores of 3 + 3, 3 + 4, 4 + 3, and 4 + 4, respectively (Table 1). All of the prostate cancers detected in this study were clinically significant. Five patients received both targeted and systematic TRUS-guided biopsy during the same section, and all of the cores from systematic biopsy showed negative results. Eight of the 10 cancer patients received a prostatectomy. The Gleason score of the final pathology was concordant with the biopsy results in five patients, upgraded in two patients, and downgraded in one patient.

3.3. PSA-related data

Age, transitional zone volume, and PSA-related data associated with the cancer-yield and noncancer-yield groups are compared in Table 2. Although the mean PSA level was higher in the cancer-yield group (mean 21.57 ng/mL; 4.89–56.33 ng/mL) as compared with the noncancer yield group (mean 11.72 ng/mL; 4.82–27.23 ng/mL), the effect size was large, resulting in differences that were not significant ($p = 0.123$). The difference in the PSA velocity between the two groups was also not significant ($p = 0.431$). Also, the transitional zone volume was larger in the noncancer-yield group ($p = 0.057$). PSATZ was significantly higher in the cancer-yield group (1.16 ng/mL/cm³; 0.25–3.15) relative to that observed in the noncancer-yield group (0.40 ng/mL/cm³; 0.11–1.63) ($p = 0.024$). A cut-off value of 0.45 ng/mL/cm³ was calculated. The area under the ROC curve was 0.841, and the sensitivity and specificity using this cut-off value were 90% and 67.6%, respectively.

3.4. Follow-up status

Immediately after the TRUS-guided biopsy procedure, only one patient experienced anal pain and bleeding during

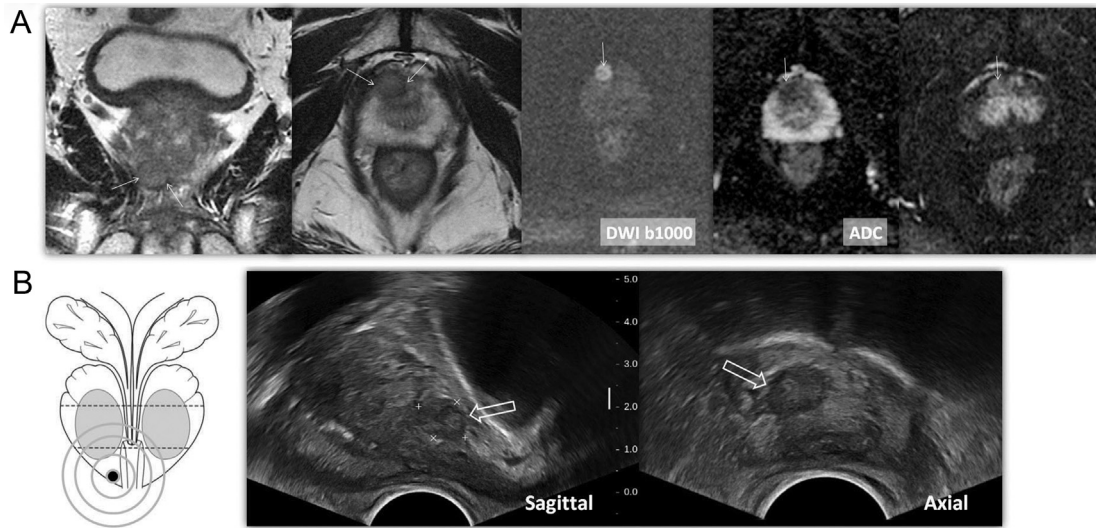


Fig. 1. A 62-year-old man with elevated PSA (14.33 mg/dL) and previous negative-systematic biopsy. (A) MRI (from left to right: T2-weighted coronal scan, T2-weighted axial scan, DWI, corresponding ADC map, and postcontrast-enhanced T1-weighted subtraction imaging) revealed a tumor nodule at right apex (arrows); and (B) transrectal ultrasound (from left to right: targeting diagram, sagittal scan, and axial scan) localized the nodule at corresponding area (open arrows). The targeted biopsy yielded prostate adenocarcinoma (Gleason score 3 + 3). The final histopathological result of radical prostatectomy was Gleason score 3 + 4, stage pT3a. ADC = apparent diffusion coefficient; DWI = diffusion-weighted imaging; MRI = magnetic resonance imaging; PSA = prostate-specific antigen.

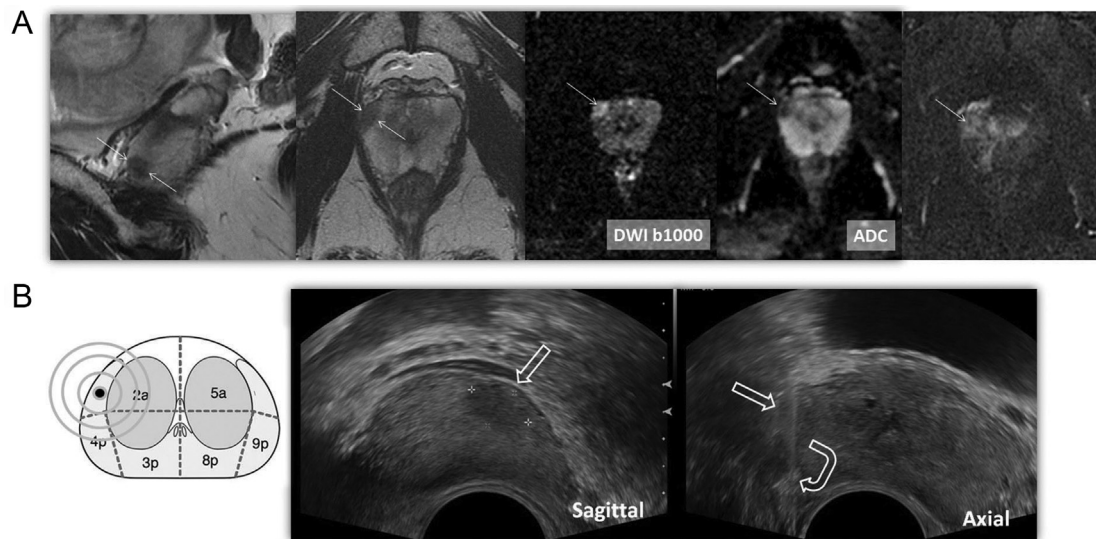


Fig. 2. A 57-year-old man with elevated PSA (4.89 mg/dL) and previous negative-systematic biopsy. (A) MRI (from left to right: T2-weighted sagittal scan, T2-weighted axial scan, DWI, corresponding ADC map, and postcontrast-enhanced T1-weighted subtraction imaging) demonstrated a suspicious lesion at the anterior horn of the right peripheral zone (arrows); and (B) transrectal ultrasound (from left to right: targeting diagram, sagittal scan, and axial scan) identified the lesion at the corresponding area (open arrows). Targeted biopsy was performed (curved open arrow: biopsy needle) and revealed prostate adenocarcinoma (Gleason score 3 + 4). The final histopathological result of radical prostatectomy was Gleason score 3 + 4, stage pT3a. ADC = apparent diffusion coefficient; DWI = diffusion-weighted imaging; MRI = magnetic resonance imaging; PSA = prostate-specific antigen.

defecation (6.7%; 1/15). None had hematuria or urinary retention. One patient (6.7%) experienced systemic infection and required intravenous antibiotics treatment.

The average follow-up duration for the 38 noncancer-yield patients was 461.5 days (244–810 days), with none of them found to have cancer during the follow-up period.

4. Discussion

The low specificity of the PSA test and the low sensitivity of TRUS-guided systematic biopsy have resulted in a high number of patients diagnosed with elevated PSA levels and negative TRUS-guided systematic biopsy results. The

Table 2
Comparison of PSA-related data between the cancer-yield and noncancer-yield groups.

	Cancer-yield group	Noncancer-yield group	<i>p</i>
Age (y)	66.5 ± 7.472	63.34 ± 6.166	0.174
PSA (ng/mL)	21.57 ± 18.07	11.72 ± 6.52	0.123
PSA velocity (ng/mL/mo.)	0.673 ± 0.57	0.398 ± 0.80	0.431
Transitional zone volume (cm ³)	22.29 ± 13.23	38.69 ± 25.55	0.057
PSA transitional zone density (ng/mL/cm ³)	1.16 ± 0.87	0.40 ± 0.32	0.024

PSA = prostate-specific antigen.

presence of malignancies remains a clinical dilemma, and when only follow-ups are arranged, this can result in tremendous anxiety among patients and increased risk of delayed diagnoses. Various techniques allowing tumor visualization and subsequent image-guided biopsies are therefore imperative.

Recent advances in MRI techniques for detecting and localizing prostate cancer have improved the aforementioned scenario. Many studies reported that MRI-guided targeted biopsies in patients with elevated PSA levels and negative systematic TRUS-guided biopsy detected cancer in 21% to 52% of patients, although the MRI protocol and guided-biopsy methods varied.^{4,10–13,15} In this study, we prospectively performed MRI scans and subsequently targeted TRUS-guided biopsy with cognitive registration. The MRI scans showed positive results in 35.4% patients, and the overall cancer-yield rate was 21%. This result substantiates the benefits of MRI-guided targeted prostate biopsy for patients with contradicting results of negative biopsies and persistently elevated PSA levels. Among the eight cancer patients in our study who underwent surgery, five had T3-stage disease and only three had T2 disease, indicating that the diagnosis solely through systematic TRUS-guided biopsy could have resulted in overlooking severe lesions and delaying treatment. Furthermore, the results of our study were consistent with previous studies reporting that systematic TRUS-guided biopsy usually misses detection of tumors located at the apex, transition zone, and anterior horns of the peripheral zone of the prostate gland.^{19–22}

There remains a concern that significant cancers may be missed if a standard systematic biopsy is omitted. Sonn et al¹⁵ studied 105 patients with elevated PSA levels and negative biopsies, and systematic biopsies were performed regardless of MRI scans, with target biopsy performed for those patients with positive MRI results. Targeted biopsy detected a higher percentage of significant cancer as compared with systematic biopsy; however, ~10% of the patients diagnosed with significant cancer showed no suspicious lesions on MR images. Siddiqui et al²³ studied 1003 patients and found that 3% yielded intermediate or high-risk disease via systematic biopsy, with no lesion detected according to mpMRI. Therefore, although mpMRI results that are negative for prostate cancer are reported to show >95% negative-predictive value for clinically significant cancer,^{24,25} there is still controversy

regarding whether a targeted biopsy can completely replace systematic biopsy. However, concurrent standard 12-core systematic biopsy and target biopsy indicates that taking >16 biopsy cores and >20 cores in cases with more than two target lesions raises the concern of increasing complications. In our study, the option of systematic biopsy was informed and discussed with the patients, with most opting for targeted biopsy only. The strategy of targeted biopsies for high-risk lesions has the advantage of obtaining fewer biopsy cores and causing fewer complications, and, therefore, has been adopted in our clinical practice. By active surveillance and further follow-ups of the noncancer-yield patients, treatment of potentially undetected cancer would not be delayed.

Degree of suspicion based on MRI scans was the most powerful predictor of significant cancer according to multivariate analysis,¹⁵ and a higher MRI-suspicion score was associated with a higher detection rate of significant prostate cancer.^{26,27} Previously, few studies on MRI-guided targeted prostate biopsy designed their own risk stratification of the lesions detected by MRI.^{15,23,27} In 2013, the ESUR published a unified scoring system called PI-RADS to establish technical and reporting standards for consistent interpretation and communication of prostate mpMRI results.¹⁶ In 2015, a refined version of PI-RADS (v2) was developed in conjunction with the American College of Radiology, which used a five-point scale to indicate the likelihood of significant prostate cancer based on mpMR findings.¹⁷ So far, limited studies have incorporated the PI-RADS (v2) scoring system for targeted biopsy.²⁸ In our study, we applied the PI-RADS (v2) assessment to the imaging analysis and found that the cancer-yield rate for score-4 lesions was much lower than that for the score-5 lesions, which agrees with results from previous reports. However, only three biopsy scores were obtained from all targeted lesions, and there may remain an increased chance of mis-targeting for smaller lesions. The existing evidence is insufficient to determine whether the lower cancer-yield rate associated with lower-risk lesions are due to mis-targeting and whether increasing the number of biopsies is necessary to yield the most significant cancer results for lesions of a lower-risk category.²⁹ Active surveillance and further follow-ups for the noncancer-yield patients are required to provide answers to these questions.

An MRI procedure can be very expensive, and routine prebiopsy MRI may be a large financial burden on the healthcare system. To avoid unnecessary biopsy and excessive use of MRI facilities, defining more strict clinical criteria for prebiopsy MRI is essential. In this study, we found that PSATZ was the most significantly different PSA-related data between the cancer-yield and noncancer-yield groups. Our results were consistent with those of Margel et al,²² suggesting that PSA density increased in patients with lesion size >1 cm as detected through MRI scans and compared with those exhibiting normal MRI results (0.15 vs. 0.07 ng/mL/cm³; *p* = 0.018). One of the major sources of serum PSA is leakage from the transition zone; therefore, the volume detected in the transition zone is strongly associated with serum PSA level.³⁰ Dividing the serum PSA level by the

transitional zone volume provides calibration to decrease the influence of BPH, thus enhancing the probability of prostate cancer existence. In this study, the cut-off value of 0.45 ng/mL/cm³ resulted in a high sensitivity of 90% for highly suspicious lesions found through MRI scans. Therefore, we recommend the measurement of transitional zone volume as a standard part of TRUS, because this may constitute a useful criterion for selecting patients for prebiopsy MRI and subsequently avoid excessive MRI use.

Different techniques associated with MRI-guided targeted biopsy are used in different institutions and dependent upon available technical and manpower resources. Direct MRI-guided targeted biopsy has been adapted for guiding biopsy procedures³¹; however, MRI is time intensive and expensive. A combination of MRI for cognitive registration and TRUS-guided biopsy is clinically practical and requires no expensive or complex techniques. Image registration between the mpMRI and ultrasound images is achieved either by fusion software or cognitive fusion. Although a study using a validated TRUS prostate-biopsy simulator reported that MRI-targeted TRUS-guided prostate biopsy using cognitive registration was inferior to software fusion,³² it was reported that software fusion and cognitive fusion do not differ significantly.^{33,34} In our experience, all lesions with PI-RADS scores of 4 or 5 could be identified through TRUS images with known MRI results. Additional verification is necessary to determine whether software fusion is helpful to yield small-lesion determination. Transperineal template prostate-mapping biopsy is another popular method for guided biopsy,^{26,35} whereas general anesthesia is required for this method; however, no comparative data are available for the aforementioned methods.

Several limitations existed for this study, with the first and major one being the small sample size. Second, only highly suspicious lesions detected through MRI received MRI-guided targeted biopsy, and systematic biopsies were not performed for all patients. Some significant cancers can potentially be missed. Last and most importantly, long-term follow-up results were not available, and the false-negative rate associated with this approach is, therefore, not available.

Acknowledgments

This study was supported by research grant of Taipei Veterans General Hospital research grant VGH103C-016.

References

1. Tseng CH. Prostate cancer mortality in Taiwanese men: increasing age-standardized trend in general population and increased risk in diabetic men. *Ann Med* 2011;**43**:142–50.
2. Margolis DJ. Multiparametric MRI for localized prostate cancer: lesion detection and staging. *Biomed Res Int* 2014;**2014**:684127.
3. Wei TC, Lin TP, Chang YH, Chen TJ, Lin AT, Chen KK. Transrectal ultrasound-guided prostate biopsy in Taiwan: a nationwide database study. *J Chin Med Assoc* 2015;**78**:662–5.
4. Futterer JJ, Verma S, Hambroek T, Yakar D, Barentsz JO. High-risk prostate cancer: value of multi-modality 3T MRI-guided biopsies after previous negative biopsies. *Abdom Imaging* 2012;**37**:892–6.
5. Kurhanewicz J, Vigneron D, Carroll P, Coakley F. Multiparametric magnetic resonance imaging in prostate cancer: present and future. *Curr Opin Urol* 2008;**18**:71–7.
6. Macura KJ. Multiparametric magnetic resonance imaging of the prostate: current status in prostate cancer detection, localization, and staging. *Semin Roentgenol* 2008;**43**:303–13.
7. Kim JK, Jang YJ, Cho G. Multidisciplinary functional MR imaging for prostate cancer. *Korean J Radiol* 2009;**10**:535–51.
8. Seitz M, Shukla-Dave A, Bjartell A, Touijer K, Sciarra A, Bastian PJ, et al. Functional magnetic resonance imaging in prostate cancer. *Eur Urol* 2009;**55**:801–14.
9. Boonsirikamchai P, Choi S, Frank SJ, Ma J, Elsayes KM, Kaur H, et al. MR imaging of prostate cancer in radiation oncology: what radiologists need to know. *Radiographics* 2013;**33**:741–61.
10. Cornelis F, Rigou G, Le Bras Y, Coutouly X, Hübner R, Yacoub M, et al. Real-time contrast-enhanced transrectal US-guided prostate biopsy: diagnostic accuracy in men with previously negative biopsy results and positive MR imaging findings. *Radiology* 2013;**269**:159–66.
11. Franiel T, Stephan C, Erbersdobler A, Dietz E, Maxeiner A, Hell N, et al. Areas suspicious for prostate cancer: MR-guided biopsy in patients with at least one transrectal US-guided biopsy with a negative finding—multiparametric MR imaging for detection and biopsy planning. *Radiology* 2011;**259**:162–72.
12. Lawrentschuk N, Fleschner N. The role of magnetic resonance imaging in targeting prostate cancer in patients with previous negative biopsies and elevated prostate-specific antigen levels. *BJU Int* 2009;**103**:730–3.
13. Roethke M, Anastasiadis AG, Lichy M, Werner M, Wagner P, Kruck S, et al. MRI-guided prostate biopsy detects clinically significant cancer: analysis of a cohort of 100 patients after previous negative TRUS biopsy. *World J Urol* 2012;**30**:213–8.
14. Scheidler J, Weores I, Brinkschmidt C, Zeitler H, Panzer S, Scharf M, et al. Diagnosis of prostate cancer in patients with persistently elevated PSA and tumor-negative biopsy in ambulatory care: performance of MR imaging in a multi-reader environment. *Rofo* 2012;**184**:130–5.
15. Sonn GA, Chang E, Natarajan S, Margolis DJ, Macairan M, Lieu P, et al. Value of targeted prostate biopsy using magnetic resonance-ultrasound fusion in men with prior negative biopsy and elevated prostate-specific antigen. *Eur Urol* 2014;**65**:809–15.
16. Barentsz JO, Richenberg J, Clements R, Choyke P, Verma S, Villeirs G, et al. ESUR prostate MR guidelines 2012. *Eur Radiol* 2012;**22**:746–57.
17. Weinreb JC, Barentsz JO, Choyke PL, Cornud F, Haider MA, Macura KJ, et al. PI-RADS Prostate Imaging – Reporting and Data System: 2015, Version 2. *Eur Urol* 2016;**69**:16–40.
18. Epstein JI, Walsh PC, Carmichael M, Brendler CB. Pathologic and clinical findings to predict tumor extent of nonpalpable (stage T1c) prostate cancer. *JAMA* 1994;**271**:368–74.
19. Hambroek T, Somford DM, Hoeks C, Bouwense SA, Huisman H, Yakar D, et al. Magnetic resonance imaging guided prostate biopsy in men with repeat negative biopsies and increased prostate specific antigen. *J Urol* 2010;**183**:520–7.
20. Lawrentschuk N, Haider MA, Daljeet N, Evans A, Toi A, Finelli A, et al. 'Prostatic evasive anterior tumours': the role of magnetic resonance imaging. *BJU Int* 2010;**105**:1231–6.
21. Lemaitre L, Puech P, Poncelet E, Bouye S, Leroy X, Biserte J, et al. Dynamic contrast-enhanced MRI of anterior prostate cancer: morphometric assessment and correlation with radical prostatectomy findings. *Eur Radiol* 2009;**19**:470–80.
22. Margel D, Yap SA, Lawrentschuk N, Klotz L, Haider M, Hersey K, et al. Impact of multiparametric endorectal coil prostate magnetic resonance imaging on disease reclassification among active surveillance candidates: a prospective cohort study. *J Urol* 2012;**187**:1247–52.
23. Siddiqui MM, Rais-Bahrami S, Turkbey B, George AK, Rothwax J, Shaker N, et al. Comparison of MR/ultrasound fusion-guided biopsy with ultrasound-guided biopsy for the diagnosis of prostate cancer. *JAMA* 2015;**313**:390–7.
24. Somford DM, Hoeks CM, Hulsbergen-van de Kaa CA, Hambroek T, Futterer JJ, Witjes JA, et al. Evaluation of diffusion-weighted MR imaging

- at inclusion in an active surveillance protocol for low-risk prostate cancer. *Invest Radiol* 2013;**48**:152–7.
25. Villers A, Puech P, Mouton D, Leroy X, Ballereau C, Lemaitre L. Dynamic contrast enhanced, pelvic phased array magnetic resonance imaging of localized prostate cancer for predicting tumor volume: correlation with radical prostatectomy findings. *J Urol* 2006;**176**:2432–7.
 26. Borkowetz A, Platzek I, Toma M, Laniado M, Baretton G, Froehner M, et al. Comparison of systematic transrectal biopsy to transperineal magnetic resonance imaging/ultrasound-fusion biopsy for the diagnosis of prostate cancer. *BJU Int* 2015;**116**:873–9.
 27. Meng X, Rosenkrantz AB, Mendhiratta N, Fenstermaker M, Huang R, Wysock JS, et al. Relationship between prebiopsy multiparametric magnetic resonance imaging (MRI), biopsy indication, and MRI-ultrasound fusion-targeted prostate biopsy outcomes. *Eur Urol* 2016;**69**:512–7.
 28. Rastinehad AR, Waingankar N, Turkbey B, Yaskiv O, Sonstegard AM, Fakhoury M, et al. Comparison of multiparametric MRI scoring systems and the impact on cancer detection in patients undergoing MR US fusion guided prostate biopsies. *PLoS One* 2015;**10**:e0143404.
 29. Yang CW, Lin TP, Huang YH, Chung HJ, Kuo JY, Huang WJ, et al. Does extended prostate needle biopsy improve the concordance of Gleason scores between biopsy and prostatectomy in the Taiwanese population? *J Chin Med Assoc* 2012;**75**:97–101.
 30. Hammerer PG, McNeal JE, Stamey TA. Correlation between serum prostate specific antigen levels and the volume of the individual glandular zones of the human prostate. *J Urol* 1995;**153**:111–4.
 31. Beyersdorff D, Winkel A, Hamm B, Lenk S, Loening SA, Taupitz M. MR imaging-guided prostate biopsy with a closed MR unit at 1.5 T: initial results. *Radiology* 2005;**234**:576–81.
 32. Cool DW, Zhang X, Romagnoli C, Izawa JJ, Romano WM, Fenster A. Evaluation of MRI-TRUS fusion versus cognitive registration accuracy for MRI-targeted, TRUS-guided prostate biopsy. *AJR Am J Roentgenol* 2015;**204**:83–91.
 33. Puech P, Rouviere O, Renard-Penna R, Villers A, Devos P, Colombel M, et al. Prostate cancer diagnosis: multiparametric MR-targeted biopsy with cognitive and transrectal US-MR fusion guidance versus systematic biopsy—prospective multicenter study. *Radiology* 2013;**268**:461–9.
 34. Valerio M, McCartan N, Freeman A, Punwani S, Emberton M, Ahmed HU. Visually directed vs. software-based targeted biopsy compared to transperineal template mapping biopsy in the detection of clinically significant prostate cancer. *Urol Oncol* 2015;**33**: 424.e9-16.
 35. Sivaraman A, Sanchez-Salas R, Barret E, Ahallal Y, Rozet F, Galiano M, et al. Transperineal template-guided mapping biopsy of the prostate. *Int J Urol* 2015;**22**:146–51.